Neuro-Oncology
26(8), 1509–1525, 2024 | https://doi.org/10.1093/neuonc/noae066 | Advance Access date 30 March 2024

The oncolytic adenovirus Delta-24-RGD in combination with ONC201 induces a potent antitumor response in pediatric high-grade and diffuse midline glioma models

Daniel de la Nava, Iker Ausejo-Mauleon, Virginia Laspidea, Marisol Gonzalez-Huarriz, Andrea Lacalle, Noelia Casares, Marta Zalacain, Lucía Marrodan, Marc García-Moure, Maria C. Ochoa, Antonio Carlos Tallon-Cobos, Reyes Hernandez-Osuna, Javier Marco-Sanz, Laasya Dhandapani, Irati Hervás-Corpión, Oren J Becher, Javad Nazarian, Sabine Mueller, Timothy N. Phoenix, Jasper van der Lugt, Mikel Hernaez, Elizabeth Guruceaga, Carl Koschmann, Sriram Venneti, Joshua E. Allen, Matthew D. Dun, Juan Fueyo, Candelaria Gomez-Manzano, Jaime Gallego Perez-Larraya, Ana Patiño-García, Sara Labiano, and Marta M. Alonso

All author affiliations are listed at the end of the article

Corresponding Author: Marta M. Alonso, PhD, Solid Tumor Program, Center for the Applied Medical Research, Pediatrics Department; Clínica Universidad de Navarra. Av. de Pío XII 55, Pamplona, Navarra, Spain (mmalonso@unav.es).

Abstract

Background. Pediatric high-grade gliomas (pHGGs), including diffuse midline gliomas (DMGs), are aggressive pediatric tumors with one of the poorest prognoses. Delta-24-RGD and ONC201 have shown promising efficacy as single agents for these tumors. However, the combination of both agents has not been evaluated.

Methods. The production of functional viruses was assessed by immunoblotting and replication assays. The antitumor effect was evaluated in a panel of human and murine pHGG and DMG cell lines. RNAseq, the seahorse stress test, mitochondrial DNA content, and γH2A.X immunofluorescence were used to perform mechanistic studies. Mouse models of both diseases were used to assess the efficacy of the combination in vivo. The tumor immune microenvironment was evaluated using flow cytometry, RNAseq, and multiplexed immunofluorescence staining.

Results. The Delta-24-RGD/ONC201 combination did not affect the virus replication capability in human pHGG and DMG models in vitro. Cytotoxicity analysis showed that the combination treatment was either synergistic or additive. Mechanistically, the combination treatment increased nuclear DNA damage and maintained the metabolic perturbation and mitochondrial damage caused by each agent alone. Delta-24-RGD/ONC201 cotreatment extended the overall survival of mice implanted with human and murine pHGG and DMG cells, independent of H3 mutation status and location. Finally, combination treatment in murine DMG models revealed a reshaping of the tumor microenvironment to a proinflammatory phenotype.

Conclusions. The Delta-24-RGD/ONC201 combination improved the efficacy compared to each agent alone in in vitro and in vivo models by potentiating nuclear DNA damage and in turn improving the antitumor (immune) response to each agent alone.

Key Points

- The D24-RGD/ONC201 combination prolonged the median survival in pHGG and DMG models.
- The D24-RGD/ONC201 antitumor effect is partly mediated by increased DNA damage.
- The D24-RGD/ONC201 combination reshaped the TME toward a proinflammatory phenotype.

Graphical Abstract

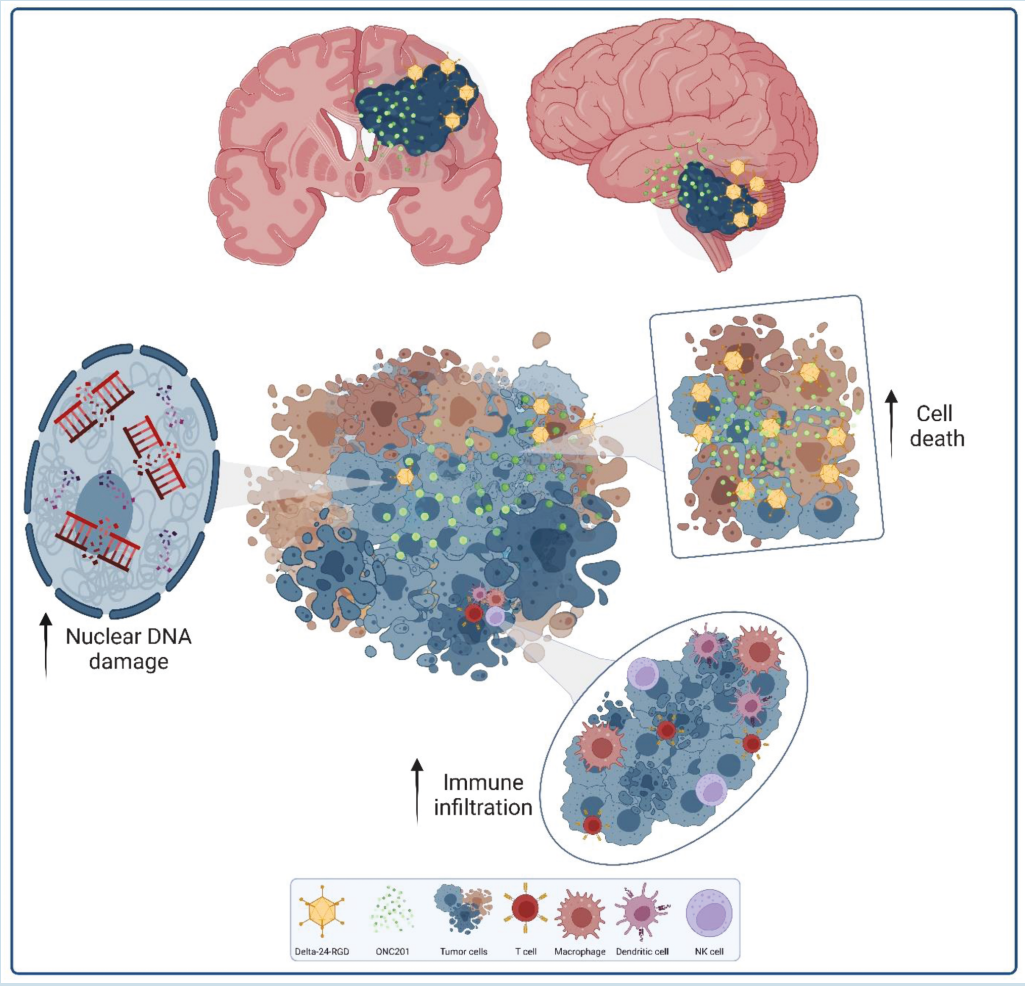

Importance of the Study

Pediatric high-grade gliomas (pHGGs), including diffuse midline gliomas (DMGs), are the most aggressive tumors with the poorest overall survival among the pediatric population. This fact underscores the urgent need for novel, alternative therapies. The oncolytic adenovirus Delta-24-RGD and the ONC201 imipridone are promising therapies but are insufficient as monotherapies. In this work, we showed that the combination of Delta-24-RGD/ONC201 was therapeutically superior to either of the single agents. The combination treatment resulted in a potent antitumor response in vitro and in vivo mediated by the intrinsic mechanism of action of each of the agents but also the synergistic increase in DNA damage that in turn increased antigen release and promoted the antitumor immune response. These results uncover the potential of the Delta-24-RGD/ONC201 combination as a treatment regimen for pHGGs and DMGs in a clinical scenario.

Tumors of the central nervous system (CNS) are the most common malignancies among children and adolescents and have the highest mortality rates of any pediatric cancer.[1] Of importance, pediatric-type diffuse high-grade gliomas (pHGGs), including diffuse midline gliomas (DMGs), are defined by a survival rate of 8–14 months, which is one of the poorest prognoses.[1–3] In the 5th and the last editions of the WHO classification for CNS tumors, pHGGs were classified based on histone H3 mutation status[4] because of their impact on epidemiology, the location of the tumor, and the disease prognosis.[5] Despite advances in imaging, neurosurgery, higher knowledge of molecular pathogenesis,

and new combinations of chemotherapy and other treatment regimes, patient outcomes and approved therapies have not changed in recent decades.[6–9] Immunotherapy, although promising in non-CNS solid tumors, has not shown efficacy in patients with pediatric brain tumors.[10] Only CAR-T-cell therapy[11,12] and virotherapy[13,14] show potential for clinical translation. However, these results are all from early-stage clinical trials and require validation in future multicentric clinical studies. Taken together, this context underscores the urgent need to propel novel therapeutic approaches that address the complex milieu of the tumor and its microenvironment.

As mentioned above, oncolytic viruses are consolidating as therapies for brain tumors due to their tumor cell selectiveness, their capability to stimulate an antitumor immune response, and their safe clinical profile, among other reasons.[15] Delta-24-RGD (DNX-2401 in the clinic), an oncolytic adenovirus derived from human adenovirus 5 (HAdV-C5), has demonstrated good antitumor efficacy in both preclinical and clinical settings in pediatric and adult gliomas.[16–21] Specifically, our group has recently demonstrated the feasibility, safety, and degree of efficacy of DNX-2401 following radiotherapy in a cohort of newly diagnosed DMG patients.[13] An enhanced immune response and remarkable T-cell recruitment were observed after treatment. Nevertheless, there is room for improvement, and combination therapy is an interesting approach.

ONC201 (dordaviprone in the clinic) is a promising small molecule that has yielded encouraging therapeutic results in clinical trials for treating H3K27M-mutant DMGs.[22] First reported as a dopamine receptor D2 (DRD2) antagonist,[23] recent research has shown that ONC201 is also an agonist of mitochondrial caseinolytic protease P (ClpP).[24–26] ONC201 induces mitochondrial damage,[24,25,27] activates the integrated stress response (ISR) signaling through activating transcription factor 4 and C/EBP homologous protein (CHOP), and induces apoptosis.[28,29] Interestingly, ONC201 also led to NK and T-cell accumulation in a colorectal tumor model.[30] ONC201 has reached the clinic in various applications for brain tumors.[27,31,32] A recent work highlighted that ONC201 treatment, following initial radiation in H3K27M-mutant DMGs, led to an encouraging response in 2 independent multisite phase II clinical trials.[27] Indeed, these results allowed for the launch of a phase III study (NCT05580562) to evaluate the efficacy in newly diagnosed patients with diffuse gliomas and H3 mutations; however, this study excluded patients with DIPG tumors. Notwithstanding the positive outcomes shown by ONC201 treatment, there is still a margin to improve the therapeutic effect of this drug.

Therefore, we aimed to elucidate whether the combination of 2 promising therapies, Delta-24-RGD and ONC201, could improve their individual therapeutic effect in preclinical models of pHGGs, including DMGs. Our data demonstrated the suitability of this combination, as it showed a better response than each agent alone in vitro and in vivo. Mechanistic studies showed that the Delta-24-RGD/ONC201 combination increased DNA damage and remodeled the tumor microenvironment (TME) toward a proinflammatory state leading to an augmented antitumor immune response. Altogether, our results reveal the potential of this treatment regime as a therapy for pHGGs, including DMGs.

Materials and Methods

Cell Lines and Culture Conditions

The CHLA-03-AA pediatric glioma cell line was obtained from American Type Culture Collection (Manassas, VA) and maintained with Dulbecco's modified Eagle's medium: nutrient mixture F-12 (DMEM/F-12; Gibco) supplemented with B-27 supplement (Gibco), basic fibroblast growth factor and epidermal growth factor (20 ng/mL Sigma–Aldrich). SJ-GBM2 was obtained from Children's Oncology Group and was maintained in Iscove's Modified Dulbecco's Medium (IMDM) supplemented with 20% fetal bovine serum (FBS), 4 mM L-glutamine and 1X insulin-transferrin-selenium ITS (Gibco). The PBT-24 cell line was derived from a patient treated at the University Clinic of Navarra[16] and was subcultured with Rosewell Park Memorial Institute medium supplemented with 10% FBS. The SF188 cell line was kindly provided by Dr. Chris Jones (Cancer Research Institute, Sutton, UK) and maintained with DMEM supplemented with 10% FBS. The human DMG cell lines were kindly provided by the following collaborators: TP54 (H3.3K27M) cells from Drs. Marie-Pierre Junier and Hervé Cheneiwess (INSERM Institute, Paris, France); the SU-DIPG IV (H3.1K27M) cell line from Dr. Michelle Monje (Stanford University, California); JHH-DIPG1 (H3.3K27M) cells from Dr. Eric Raabe (John Hopkins University, Baltimore); HSJD-DIPG-007 (H3.3K27M) cells from Dr. Angel Montero-Carcaboso (Hospital Sant Joan de Déu, Barcelona); and the SU-DIPG-XIIIp* (H3.3K27M) cell line from Dr. Carl Koschmann (University of Michigan, Ann Arbor). These cell lines were maintained as neurospheres cultured in specialized medium for the expansion of human neural stem and progenitor cells (NeuroCultTM NS-A Proliferation Kit, #05751, STEMCELL Technologies), supplemented with basic fibroblast growth factor and epidermal growth factor (20 ng/mL Sigma–Aldrich). The human DMG SF8628 cell line was obtained from Millipore (Sigma Aldrich) and was subcultured with DMEM supplemented with 10% FBS and 2 mM L-glutamine (Gibco). NP53 and XFM murine DMG cells were kindly provided by Dr. Oren Becher (Mount Sinai). Both cell lines were obtained from DMG tumors from genetically modified mice[33,34] and were maintained with DMEM supplemented with 10% FBS. The intrauterine electroporation (IUE)-derived cell lines 24D-1, 26B-7, and 26C-7 were a kind gift from Timothy N. Phoenix (Cincinnati Children's Hospital Medical Center, Cincinnati). These cell lines contain dominant-negative p53 (DN-p53), $PDGFRA^{D842V}$, and, either H3.3 WT (24D-1), H3.3K27M (26B-7), or H3.1K27M/$ACVR1^{G328V}$ (26C-7).[35] All media were supplemented with 1% penicillin/streptomycin. HEK293 cells were used for viral titration. All cell lines were maintained in a humidified atmosphere containing 5% CO_2 at 37°C, routinely tested for mycoplasma (Mycoalert mycoplasma detection kit; Lonza), and authenticated at the CIMA Genomic Core Facility (Pamplona, Spain) using DNA profiling.

Animal Studies

Ethical approval for the animal studies was granted through the Animal Ethical Committee of the University of Navarra

(CEEA; Comité Ético de Experimentación Animal) under the protocols CEEA/064-20 and CEEA/065-20. All animal procedures were performed in accordance with the institutional, regional, and national laboratory animal research guidelines. Efforts were made to reduce the number of mice used according to the 3R principles to minimize animal suffering.

For the orthotopic supratentorial model, CHLA-03-AA (5×10^5) cells were injected into the striatum of athymic mice. For human DMG tumors, TP54 (5×10^5) and SU-DIPG-XIIIp* (3×10^5) cells were injected into the pons of BALB/c nude and NSG mice, respectively. Murine DMG tumors were developed by injecting XFM (1×10^3) cells into the pons of BALB/c mice, NP53 (1×10^4) cells into NP53$^{fl/fl}$ transgenic mice,[33] and 24D-1 and 26C-7 (2.5×10^5) cells into C57BL/6 mice. The cells were implanted in 2–5 µL of uncomplemented media. Then, the animals were randomly assigned to each experimental group. Delta-24-RGD was administered intratumorally after cell implantation. ONC201 dissolved in distilled H_2O was administered by oral gavage at the indicated dosages once per week. ONC201 was kindly provided by Chimerix (Durham).

Statistical Analysis and Illustration Design

Data are presented as the mean ± SEM. Dose–response curves for ONC201 were obtained by nonlinear regression. The synergistic effect was calculated using the Highest Single Agent (HSA) formula in SynergyFinder.[36] Comparisons among groups were evaluated using the Mann–Whitney test (for viral replication assays) and 1/2-way ANOVA (for multiple comparisons). A P value < .05 was considered significant. Survival rates were compared using a log-rank test (Mantel–Cox) and represented as Kaplan–Meier plots. All data were analyzed using GraphPad Prism 10 (Statistical Software for Science, RRID: SCR_002798). ns, $P > .05$; *$P < .05$; **$P < .01$; ***$P < .001$; ****$P < .0001$.

Illustrations were created using BioRender.com.

Results

The combination of ONC201 with Delta-24-RGD results in a superior antitumor effect compared to that of either treatment alone in human pHGG and DMG cell lines.

As recent preclinical and clinical studies have shown that pHGG and DMG tumors are sensitive to ONC201,[24,27,37] we decided to confirm the antitumor effect of ONC201 in a battery of H3-WT pHGG (CHLA-03-AA, PBT-24, SJ-GBM2, and SF188) and H3K27M DMG (SF8628, TP54, SU-DIPG IV, HSJD-DIPG007, and JHH-DIPG-1) cell lines, which showed IC_{50} values in the micromolar range (Supplementary Figure S1A). As the goal of this work was to maximize the therapeutic effect of ONC201 in combination with the oncolytic virus Delta-24-RGD, we first ruled out the potential negative effects of ONC201 on the replication capability of the virus due to its mechanism of action. Although the addition of ONC201 IC_{50} to viral treatment led to a slight reduction in the levels of the early (E1A) and late (Fiber) viral proteins (Figure 1A, Supplementary Figure S1B, C, and D), evaluation of viral replication after ONC201 addition showed no drug interference with the production of functional viruses (Figure 1B, Supplementary Figure S1E). These data indicate that although ONC201 abrogates growth signals and mitochondrial metabolism and could thus potentially interfere with the viral cycle, this effect is not sufficient to diminish viral replication, which suggests that this combination could be therapeutically viable. Importantly, combination treatment induced a synergistic or additive antitumor effect in all cell lines tested regardless of H3 mutation status (Figure 1C–D). The HSA algorithm was used to assess the potential additivity (0 < HSA overall score < 10) or synergy (10 < HSA overall score).[36] The Delta-24-RGD/ONC201 combination in pHGG cell lines was additive (SJ-GBM2: HSA = 6.66) or synergistic (CHLA-03-AA: HSA = 12.85; SF188: HSA = 28.12). Similar results were obtained in the DMG cell lines evaluated, with additivity in TP54 (HSA = 3.30) and synergy in SF8628 (HSA = 19.27) and SU-DIPG IV (HSA = 10.19; Figure 1D).

Collectively, these data showed the feasibility of the Delta-24-RGD/ONC201 combination, with no negative effects on adenovirus replication capability by ONC201. Additionally, the results proved that the Delta-24-RGD/ONC201 combination is either synergistic or additive, and the combination led to better responses than each treatment alone in vitro.

The Delta-24-RGD/ONC201 Combination Conserves the Metabolic and Mitochondrial Disruptions and Exacerbates DNA Damage

To better understand the mechanism of action of this combination, we performed RNAseq analysis after the indicated treatments. Two cell lines per type of tumor were included (pHGG: CHLA-03-AA, SJ-GBM2; and DMG: TP54, SU-DIPG IV; Figure 2A-C, Supplementary Figure S2A). In both disease models, genes related to the immune response were differentially expressed in the presence of Delta-24-RGD, whereas ONC201 led to changes in the expression of genes that regulate apoptosis, ISR, and nuclear DNA damage. Importantly, the combination conserved all of these changes (Figure 2A). Gene sets analyses showed that the Delta-24-RGD/ONC201 combination has a higher impact than monotherapies to downregulate transcriptional signatures of pathways related to tumor development and cell proliferation (Supplementary Figure S2A). We also compared the effects of the Delta-24-RGD/ONC201 combination with the individual treatments (Figure 2B). pHGG cells, following combination treatment, differentially regulated the ISR and mitochondrial homeostasis. In contrast, combination treatment in DMG cells altered the regulation of phosphatidylinositol 3-kinase activity and the nuclear DNA damage response (Figure 2B). These data suggest that Delta-24-RGD and ONC201 do not interfere with each other's transcriptional reprogramming as single agents in addition to their additive antitumor and viral responses when used in combination. Additionally, we identified that DMG cells treated with the combination showed a significant reduction of IGF1/IGF1R and PDGF pathways (Figure 2C), which have been previously

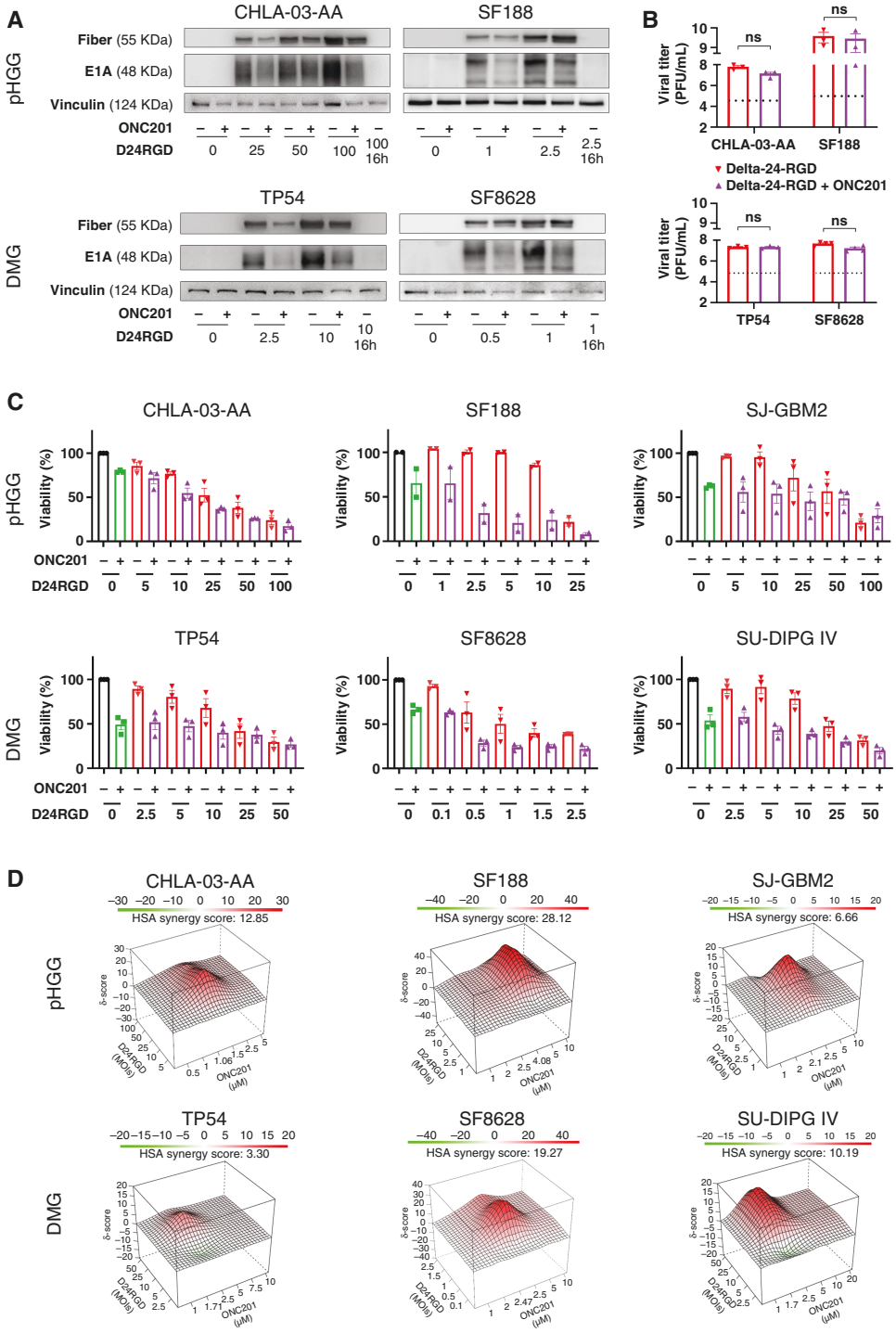

Figure 1. (A) The levels of early (E1A) and late (Fiber) viral proteins in the absence/presence of ONC201 and Delta-24-RGD in human pHGG (CHLA-03-AA, SF188) and DMG (TP54, SF8628) cells were assessed by immunoblotting 72 hours after treatment. Delta-24-RGD numbers indicate the multiplicity of infection (MOI) used. ONC201 treatment was given at the IC_{50} dosage. (B) Total infection titers of Delta-24-RGD in the absence/presence of ONC201 72 hours after treatment in pHGG (CHLA-03-AA, SF188) and DMG (TP54, SF8628) cells were quantified by an anti-hexon staining-based method. Cells were treated at the following Delta-24-RGD dosages: CHLA-03-AA: 5 PFU/cell; SF188: 2.5 PFU/cell; TP54: 10 PFU/cell; and SF8628: 0.5 PFU/cell. ONC201 treatment was given at the IC_{50} dosage. Horizontal dotted lines indicate the input virus. Data are shown in logarithm format and as the mean ± SEM. At least 3 biological replicates were performed for each condition. The Mann–Whitney test was performed for statistical analysis. ns, not significant. (C) Effects on viability of Delta-24-RGD ± ONC201 in human pHGG (CHLA-03-AA, SF188, and SJ-GBM2) and DMG (TP54, SF8628, and SU-DIPG IV) cells. Cells were treated with increasing MOIs of Delta-24-RGD in the absence or presence of ONC201 (at $IC_{75\text{-}50}$). At least 2 biological replicates were performed for each cell line. (D) 3D-synergy maps of data from C, analyzed by the Highest Single Agent (HSA) logarithm. An HSA overall score > 10 represents strong synergy; a 0 < HSA overall score < 10 represents additivity.

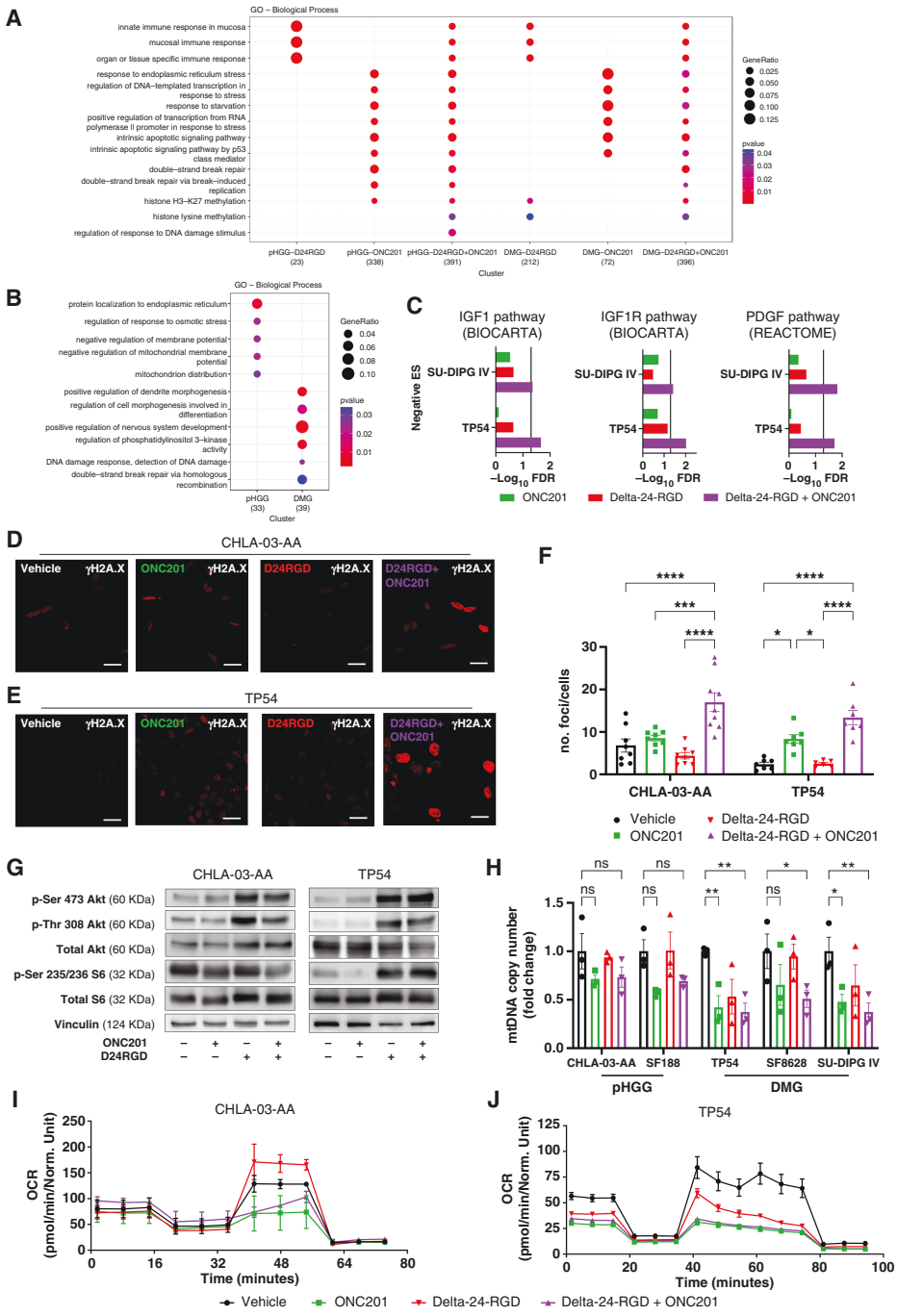

Figure 2. (A) Gene ontology families enriched in the human pHGG and DMG cell lines following Delta-24-RGD, ONC201, and combination treatment compared with vehicle. The results were obtained from RNAseq data (GSE255972). (B) Gene ontology families enriched in the Delta-24-RGD/ONC201 combination group compared with each individual treatment group in human pHGG and DMG cell lines. (C) GSEA (negative enriched) of transcriptomic signatures in human DMG cell lines after ONC201 and/or Delta-24-RGD treatment. Vertical line indicates statistical significance ($-\text{Log}_{10}$ 0.05). (D) and (E) Representative immunofluorescence images of γH2AX levels in CHLA-03-AA (D) and TP54 (E) cells 48 hours after Delta-24-RGD and/or ONC201 treatment. Scale bars: 25 μm. (F) Quantification of no. foci/no. cells from D and E. Data are shown as the mean ± SEM. At least 6 independent images were quantified from 2 experimental replicates. One-way ANOVA was performed for statistical analysis. *$P < .05$, ***$P < .001$, ****$P < .0001$. G. Assessment of the mTORC1 pathway in pHGG (CHLA-03-AA) and DMG (TP54) cell lines 48 hours after Delta-24-RGD, ONC201 or combination treatment. H. Relative mtDNA level in pHGG (CHLA-03, SF188) and DMG (TP54, SF8628, SU-DIPG IV) cells for 24 hours after ONC201 and/or Delta-24-RGD treatment. Data are shown normalized versus "vehicle" and as the mean ± SEM. Three biological replicates were performed for each cell line. Two-way ANOVA was performed for statistical analysis. *$P < .05$, **$P < .01$. Cells were treated with Delta-24-RGD at the IC_{50} of ONC201 and 10 PFU/cell for Figure 2D to H. I and J. Seahorse extracellular flux analysis showing the OCR in CHLA-03-AA (I) and TP54 (J) cells 24 hours after ONC201 and/or Delta-24-RGD treatment. Three experimental replicates were performed for each condition. The Delta-24-RGD dosage was 25 PFU/cell (CHLA-03-AA) or 15 PFU/cell (TP54), and ONC201 was given at the IC_{50} for both cell lines.

described as potential targets for recent alternative therapeutic approaches.[38,39]

Intriguingly, RNAseq data revealed that the combination treatment increased nuclear DNA damage, suggesting a possible mechanism underlying the enhanced antitumor effect (Figure 2A–B). Interestingly, adenoviruses switch off nuclear DNA damage repair machinery early after infection to avoid the recognition of single viral DNA ends by the cell and to facilitate replication.[40] Therefore, we measured nuclear DNA damage based on the relative levels of phospho-histone H2A.X (γH2A.X) by immunofluorescence microscopy, and we quantified the no. foci/no. cells ratio and the integrated density. ONC201 tended to slightly increase DNA damage in both disease models, whereas Delta-24-RGD infection had no significant impact on γH2A.X levels (Figure 2D–E, Supplementary Figure S2B–E). However, cotreatment with Delta-24-RGD and ONC201 resulted in increased γH2A.X levels, higher than that induced by each agent alone, indicating more DNA damage.

To delve into the mechanism of action of the combination and because ONC201 was described as an indirect inhibitor of the cell proliferation and protein production mTORC1 pathway,[29,30] we evaluated the effect of Delta-24-RGD/ONC201 treatment on this metabolic pathway (Figure 2G, Supplementary Figure S2F). We observed that ONC201 at the IC_{50} decreased the phosphorylation of the mTORC1 target S6 ribosomal protein but did not change p-Ser 473 and p-Thr 308 Akt phosphorylation. Meanwhile, Delta-24-RGD infection activated mTORC1 signaling, which increased phosphorylation at p-Ser 473, p-Thr 308 Akt, and the S6 ribosomal protein, probably to expand the production of viral proteins. Indeed, this effect was maintained even in the presence of ONC201, which demonstrated the potent effect of Delta-24-RGD on this signaling pathway.

Similarly, as one of the main mechanisms underlying the efficacy of ONC201 is the perturbation of mitochondrial respiratory capacity,[24,25] we investigated whether Delta-24-RGD could interfere with this process. First, we quantified the levels of mtDNA to more precisely characterize the role of the mitochondria in the combination treatment efficacy (Figure 2H). Delta-24-RGD alone did not affect the mtDNA copy number. In contrast, ONC201, alone or combined with Delta-24-RGD, decreased the mtDNA level, confirming mitochondrial damage. We also performed a Seahorse analysis to measure respiratory capacity. As previously described,[24,25,27] ONC201 altered the OCR in all cells evaluated meanwhile Delta-24-RGD treatment did not produce significant changes (Figure 2I-J; Supplementary Figure S3A). ONC201 and the combination treatment increased ECAR (Supplementary Figure S3B) and decreased the basal oxygen consumption rate, ATP-linked respiration, maximal respiration capacity, spare capacity, and nonmitochondrial respiration (Supplementary Figure S3C–E). Altogether, these data demonstrate that the mitochondrial perturbation by ONC201 is maintained in the presence of Delta-24-RGD.

To summarize, these data showed that in vitro, Delta-24-RGD infection reprograms the cells while ISR, apoptosis, and nuclear DNA damage are induced by ONC201. Of importance, the combination treatment does not interfere with the effect of the single agents alone.

Delta-24-RGD/ONC201 Cotreatment has a Superior Antitumoral Effect in Orthotopic Human Models of pHGG and DMG

Due to the encouraging results obtained in vitro, we evaluated the in vivo efficacy of this combination in xenograft human pHGG (CHLA-03-AA) and DMG (TP54 and SU-DIPG-XIIIp*) models. Cells were engrafted orthotopically, and several days later, depending on the kinetics of the model, mice were treated intratumorally with a single dose of Delta-24-RGD (10^7 pfu) followed by the administration of ONC201 (125 mg/kg, once a week, o.g.; Figure 3A). The treatment schedule was designed in a way that could be reproduced in a clinical scenario. Although both agents have been demonstrated to be safe in clinical trials as single agents,[13,27] their safety profile, when used in combination, has not yet been established. Thus, we evaluated a battery of toxicity parameters (including hemogram, biochemistry, and pathology) to rule out potential negative effects of the combination in human and murine models. As expected, the Delta-24-RGD/ONC201 combination proved to be safe in both animal models, showing no significant differences against vehicle-treated mice in any of the parameters evaluated (Supplementary Figure S4–5). Hemogram analyses showed no differences in cell count (white, red, or platelets) among treatment groups (Supplementary Figure S4A–B and S5A–B). Additionally, hepatic, pancreatic, and renal function biochemical analyses after treatment showed normal (Supplementary Figure S4C and S5C). Liver anatomopathological analyses to detect histological changes induced by the combination showed normal anatomy and no expression of E1A viral protein in any of the models (Supplementary Figure S4D and S5D).

Then, we investigated whether Delta-24-RGD would replicate and persist in the tumor after ONC201 administration in both disease models (human xenografts). Thus, animals were treated with the combination of Delta-24-RGD (single dose) followed by 3 doses of ONC201 and sacrificed one day after the last dose of drug (Figure 3A). We confirmed E1A (early viral protein) and hexon (late viral protein) staining in Delta-24-RGD-treated mice, independent of whether animals were additionally treated with vehicle or ONC201 (Figure 3B, S6A-B), indicating that ONC201 does not interfere with in vivo viral infection and replication capability. We also validated that ONC201 reached the tumor in our models as a decreased staining for succinate dehydrogenase complex subunit A (SDHA) was observed in the ONC201-treated groups, with remarkable zones without SDHA staining as other groups checked.[37] Surprisingly, Delta-24-RGD produces a similar decrease (Figure 3C-D, Supplementary Figure S6C). Further experiments would be needed to understand the biological meaning of this finding.

Next, we evaluated the efficacy of the combination in pHGG and DMG orthotopic models. In the pHGG model (CHLA-03-AA cell line, H3-WT), ONC201 led to a survival advantage, but without a significant difference (vehicle = 48 days, $n = 9$; ONC201 = 54.5 days, $n = 6$, $P = .172$). Delta-24-RGD treatment improved survival (vehicle vs. Delta-24-RGD = 62 days, $n = 8$; $P = .016$), whereas the combination of both agents significantly prolonged the survival of the

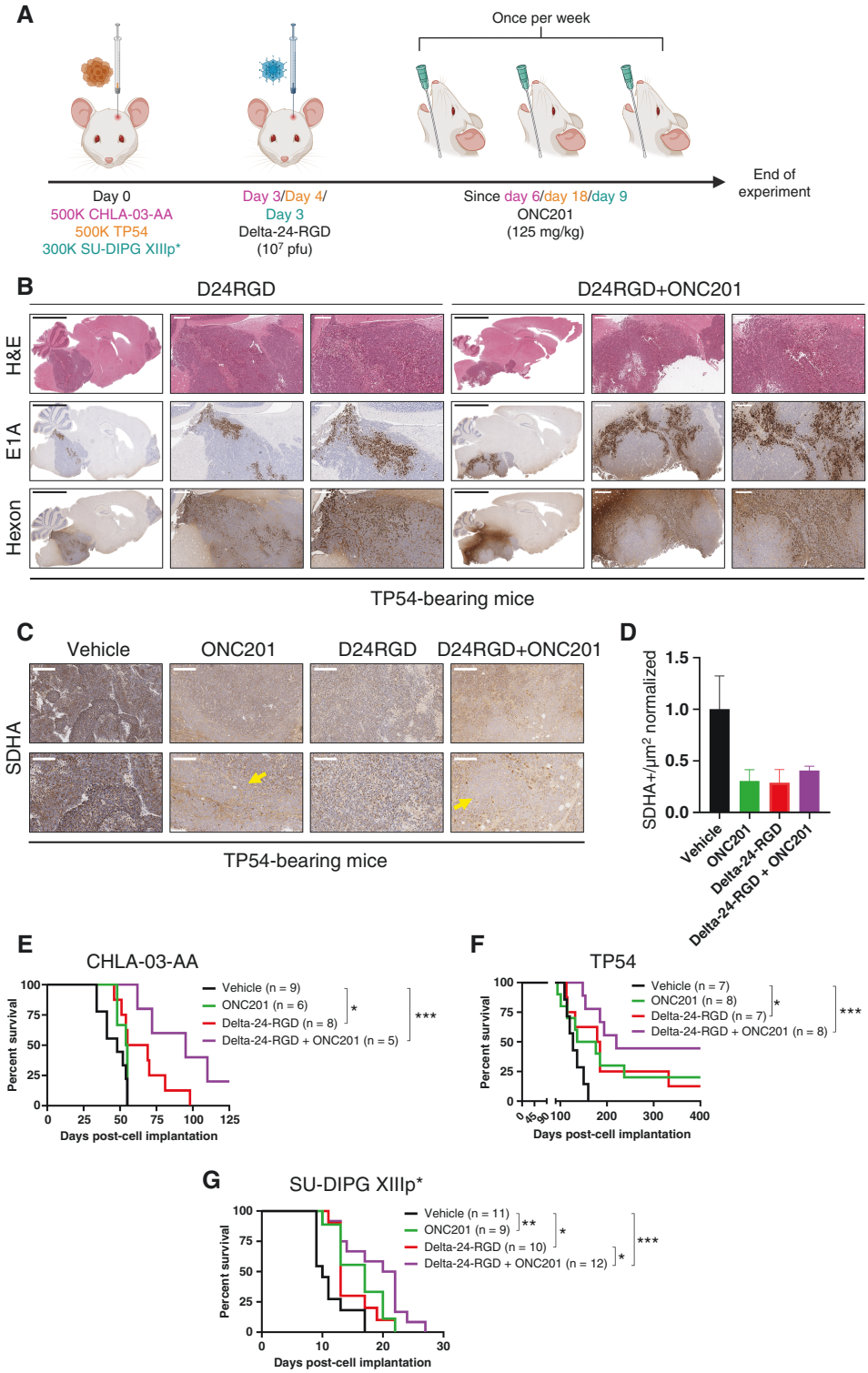

Figure 3. (A) Treatment schedule for immunosuppressed, human orthotopic-bearing mouse models (CHLA-03-AA, TP54, and SU-DIPG-XIIIp*). (B) Representative immunostaining images of brain samples from TP54-bearing mice at the sacrifice time. H&E was used to confirm tumor presence, and E1A and Hexon were used as adenovirus markers. Scale bars: 3 mm, 500 µm and 250 µm. (C) Representative images of SDHA staining from TP54-bearing mice at the sacrifice time. Scale bars: 300 µm (upper panels), and 150 µm (bottom panels). D. Quantification of SDHA staining in TP54-bearing mice and represented as SDHA+/µm^2 normalized ratio. Arrows indicate regions without SDHA staining. Scale bar: 200 µm. (E), (F) and (G). Survival curve analysis after cell implantation following the sacrifice of CHLA-03-AA (E), TP54 (F), and SU-DIPG-XIIIp*(G)-bearing mice. The log-rank (Mantel–Cox) test was performed for statistical analysis. The numbers of mice in each group appear in brackets. *$P < .05$, **$P < .01$, ***$P < .001$.

treated animals and one mouse of this group resulted in a long-term survivor (vehicle vs. Delta-24-RGD/ONC201 = 95 days, $n = 5$; $P = .0008$; Figure 3E, Supplementary Figure S7A). The DMG model TP54 (H3.3mut) showed similar results (Figure 3F, Supplementary Figure S7B), with single ONC201 or Delta-24-RGD treatment leading to an increase in the median survival time of the mice (vehicle = 127 days, $n = 7$; ONC201 = 156 days, $n = 8$, $P = .099$; Delta-24-RGD = 182 days, $n = 7$, $P = .033$), but again, the Delta-24-RGD/ONC201 combination showed a better survival advantage (220 days, $P < .0005$). All 3 treatment regimens led to long-term survival in this model: ONC201 (2 out of 10; 20%), Delta-24-RGD (1 out of 8; 12.5%), and Delta-24-RGD/ONC201 (4 out of 9; 44.4%; Figure 3F). Immunohistochemical analyses of this model after treatment showed a decrease in proliferation and an increase in apoptosis when both agents were combined (Supplementary Figure S6D). An additional DMG model of SU-DIPG-XIIIp* (H3.3mut)-bearing mice were tested with the proposed treatment regime (Figure 3G). Once again, ONC201 and Delta-24-RGD as single agents increased the median overall survival time of treated mice (vehicle = 10 days, $n = 11$, ONC201 = 17 days, $n = 9$, $P = .0081$; Delta-24-RGD = 13 days, $n = 10$, $P = .014$). Importantly, the combination regime led to a superior antitumor response (21 days, $n = 12$; vs. vehicle, $P = .0003$; vs. Delta-24-RGD, $P = .0285$; Supplementary Figure S7C). There were no long-term survivors in this model. During the experiment, weight changes were evaluated as a surrogate toxicity marker. Weight loss was not observed after treatment with each agent alone or in combination in any of the models (Supplementary Figure S7D).

Overall, these data proved the feasibility of the Delta-24-RGD/ONC201 treatment regime in an immunosuppressed in vivo context. No toxicities were associated with the combination treatment, and we observed improved antitumoral responses in both pHGG and DMG models.

The Delta-24-RGD/ONC201 Combination Maintains Its Effects in Murine DMG Cell Lines

As both ONC201[30,32] and Delta-24-RGD[13,16,19] are able to modulate the immune system, we next assessed the efficacy of the combination treatment in immunocompetent DMG models. Thus, we used XFM (H3-WT)/NP53 (H3.3mut) cell lines, which were derived from pons tumors of genetically modified mice,[33,34] and 24D-1 (H3-WT)/26B-7 (H3.3mut)/26C-7 (H3.1mut) cell lines, which were derived from tumors in IUE models.[35]

First, we assessed the conserved homology of ONC201 target proteins in mice and humans. In silico analyses showed that both CLPP and DRD2 are highly conserved (86.76% and 95.71%, respectively) in both species, suggesting the suitability of using ONC201 in murine DMG cells (Supplementary Figure S8A–B). We conducted similar in vitro experiments as we did previously with human cell lines and we confirmed that ONC201 affected the viability of murine DMG cells (Supplementary Figure S8C). IC_{50} concentrations are provided in Supplementary Figure S8C. We could detect the expression of the E1A and Fiber viral proteins even in the presence of ONC201 (Figure 4A, Supplementary Figure S8D–F), although as expected, the virus did not replicate in this model since adenoviruses are species-specific[41] (Figure 4B). Based on the HSA algorithm,[36] the Delta-24-RGD/ONC201 combination was either additive for XFM (HSA overall score = 2.64), 24D-1 (HSA overall score = 7.69) and 26B-7 (HSA = 2.54) or synergistic for NP53 (HSA overall score = 11.83) and 26C-7 (HSA overall score = 11.48; Figure 4C–D). Nuclear DNA damage was also increased in the presence of ONC201 and, similar to the effects in the human cell lines, it was further potentiated when ONC201 was combined with Delta-24-RGD (Figure 4E–F, Supplementary Figure S8G).

The efficacy of the Delta-24-RGD/ONC201 combination was also evaluated in the H3-WT and H3K27M DMG murine models. We followed a similar schedule to that previously proposed (Supplementary Figure S9A). XFM-bearing mice (H3-WT) only presented an increase in median overall survival following Delta-24-RGD/ONC201 treatment (vehicle = 11 days, $n = 8$; Delta-24-RGD/ONC201 = 15 days, $n = 9$, $P = .0273$; Figure 4G, Supplementary Figure S9B). The Delta-24-RGD/ONC201 combination improved overall survival in the 24D-1 tumor-bearing mice model (65 days, $n = 12$; vs. vehicle, $P = .0003$; vs. ONC201, $P = .0194$; vs. Delta-24-RGD, $P = .1243$; Figure 4H, Supplementary Figure S9C). In this model, ONC201 as a single agent did not significantly increase overall survival compared with the control group (vehicle = 56.5 days, $n = 10$; ONC201 = 61 days, $n = 11$, $P = .134$), while Delta-24-RGD-treated mice showed a slight but significant difference (61 days, $n = 12$; $P = .024$). Regarding the H3mut models, the survival of NP53-bearing mice was extended following treatment with ONC201 (vehicle = 19.5 days, $n = 10$; ONC201 = 22 days, $n = 11$; $P = .0447$) or Delta-24-RGD alone (21 days, $n = 12$; $P = .0586$). The Delta-24-RGD/ONC201 regimen slightly improved the effect of each agent alone (25 days, $n = 11$; $P = .0024$; Figure 4I, Supplementary Figure S9D). We also evaluated the effect of the treatments in the 26C-7 model. ONC201 (51.5 days, $n = 10$; $P = .01$), Delta-24-RGD (50 days, $n = 11$; $P < .05$), and Delta-24-RGD/ONC201 (56.5 days, $n = 12$; $P = .0002$) treatment improved overall survival in comparison with the vehicle group (46 days, $n = 11$; Figure 4J, Supplementary Figure S9E). Importantly, the combination regime showed a superior effect compared to each treatment alone (vs. vehicle, $P = .0002$; vs. ONC201, $P = .0205$; vs. Delta-24-RGD, $P = .0473$; Supplementary Figure S9E). The treatments did not lead to long-term survivors except for one mouse in the NP53-bearing model.

Altogether, our data demonstrated that the Delta-24-RDG/ONC201 combination retained the efficacy displayed in human cells in a battery of murine DMG models in vitro. Additionally, the combination is feasible in immunocompetent in vivo models and showed a modest but better response; this difference can partially be explained by the ineffective replication of adenovirus serotype 5 in murine models.[41]

The Delta-24-RGD/ONC201 Combination Induces Proinflammatory Remodeling of the Tumor Microenvironment

As the combination treatment showed a therapeutic advantage in immunocompetent models, we wanted to

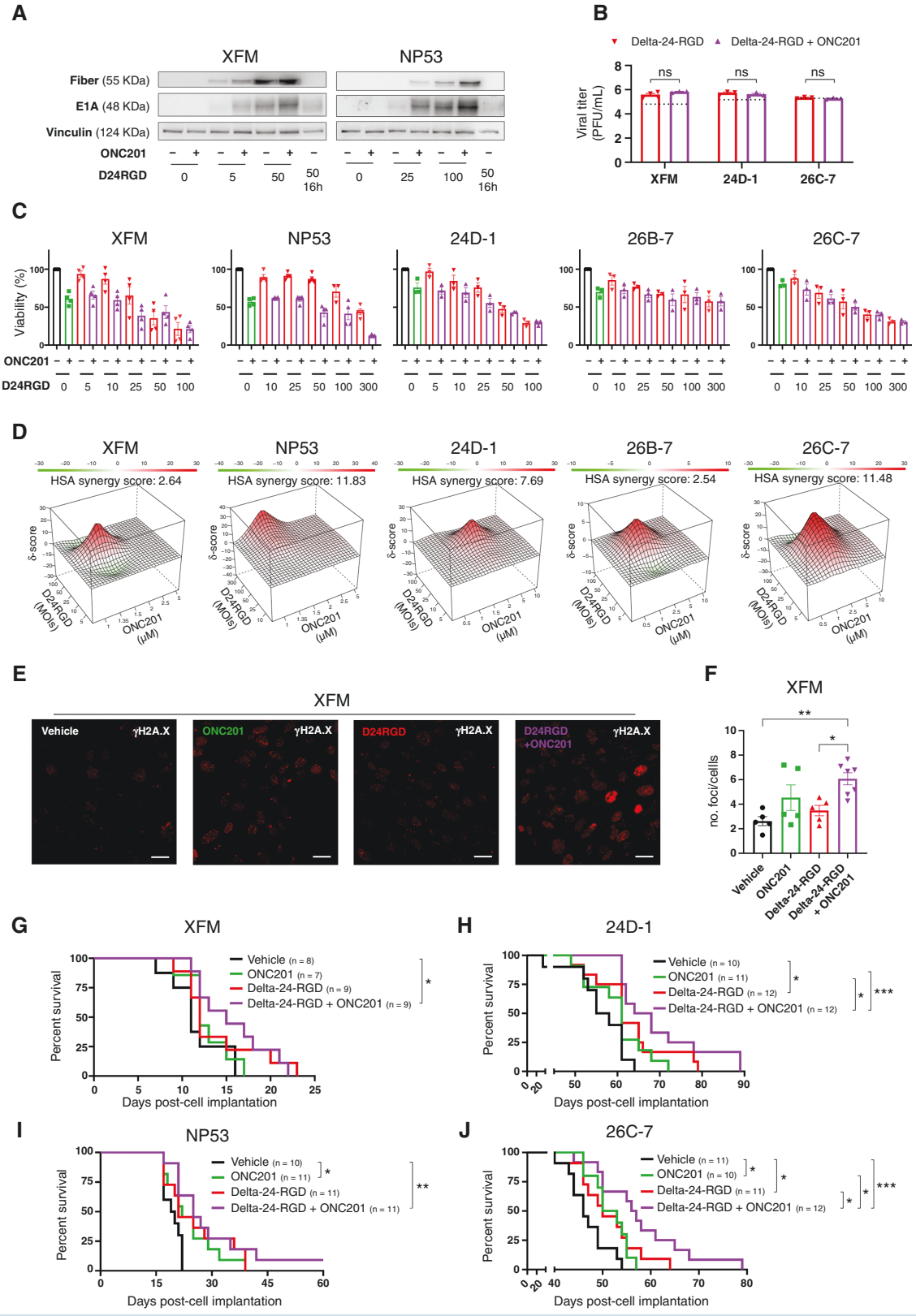

Figure 4. (A) Assessment of the levels of early (E1A) and late (Fiber) viral proteins in murine DMG (XFM or NP53) cells in the absence/presence of ONC201 following Delta-24-RGD treatment by immunoblotting. Delta-24-RGD numbers indicate the multiplicity of infections used. ONC201 treatment was given at the IC_{50} dosage. (B) Quantification of total infection titers of Delta-24-RGD in XFM, 24D-1, and 26C-7 cells by an anti-hexon staining-based method in the absence/presence of ONC201. Cells were treated with the IC_{50} of ONC201 and 100 PFU/cell Delta-24-RGD. The

horizontal dotted line indicates the input virus. Data are shown in logarithm format and as the mean ± SEM. At least 3 biological replicates were performed for each condition. The Mann–Whitney test was performed for statistical analysis. ns, not significant. (C) Effects on viability of Delta-24-RGD ± ONC201 in murine DMG (XFM, NP53, 24D-1, 26B-7, and 26C-7) cells. Cells were treated with an increasing PFU/cell Delta-24-RGD in the absence and presence of ONC201 (at $IC_{75\text{-}50}$). At least 3 biological replicates were performed for each cell line. (D) 3D-synergy maps of data from C, as analyzed by the HSA logarithm. An HSA overall score > 10 represents strong synergy; 0 < HSA overall score < 10 represents additivity. (E) Representative immunofluorescence images of γH2AX in XFM cells 48 hours after Delta-24-RGD and/or ONC201 treatment. The Delta-24-RGD dosage was 10 PFU/cell, and ONC201 was given at the IC_{50}. Scale bars: 25 μm. (F) Quantification of no. foci/no. cells from (E) Data are shown as the mean ± SEM. At least 5 independent images were quantified from 2 experimental replicates. One-way ANOVA was performed for statistical analysis. *$P < .05$, **$P < .01$. G, H, I, and J. Survival curve analysis after cell implantation following the sacrifice of XFM-(G), 24D-1-(H) NP53-(I), and 26C-7-(J) mice, respectively. The log-rank (Mantel–Cox) test was performed for statistical analysis. The numbers of mice in each group is shown in brackets. *$P < .05$, **$P < .01$, ***$P < .001$.

characterize the contribution of the combination to the antitumor immune response. Thus, we conducted a short-term experiment with a similar treatment schedule as the survival experiment (Supplementary Figure S10A), and flow cytometry analyses were performed (Supplementary Figure S10B; gating strategy). We observed that Delta-24-RGD administration alone or in combination with ONC201, increased the abundance of immune infiltrate ($CD45^+$ cells) in the tumors compared with that of vehicle-treated mice ($P = .0123$ and $P < .0001$, respectively), whereas ONC201-treated mice showed a nonsignificant increase in the number of immune cells ($P = .4301$; Figure 5A–B). Interestingly, we found robust recruitment of lymphoid and myeloid lineage cells following combination treatment (Figure 5C–E). Total $CD3^+$ T cells and, specifically, $CD4^+$, $CD8^+$, and regulatory T cells (Treg; $CD4^+Foxp3^+$), were increased in the combination group compared with the vehicle and ONC201 groups (Figure 5C). NK cells ($TCRb^-NKp46^+$) were specifically increased following Delta-24-RGD/ONC201 treatment compared with that following single treatments ($P < .0001$, $P = .0057$ and $P = .0302$ for vehicle, ONC201, and Delta-24-RGD, respectively; Figure 5C). No differences were found in the amount of B-cell infiltration in the tumor (Figure 5C). Regarding the myeloid compartment, only Delta-24-RGD/ONC201 treatment induced significant recruitment of monocytes, macrophages, microglia, and granulocytes, as well as dendritic cells (Figure 5C–D). We confirmed the increase in the infiltration into the tumor using multispectral immunofluorescence (Figure 5F). We also analyzed the impact of the combination treatment on the peripheral blood cell populations (same time point as tumor infiltrate). No differences were found in the immune populations, except for a decrease in NK cells with either treatment or in combination (Supplementary Figure S11), which was surprising due to the previous reports regarding ONC201 effect on this population.[30] We also isolated splenocytes from treated DMG-bearing mice and cocultured them with either mock-infected or Delta-24-RGD-infected cells for 24 hours IFN-γ producing cells were significantly more abundant in splenocytes treated with Delta-24-RGD in the presence or absence of ONC201 cotreatment (Supplementary Figure S12A).

After confirming a relevant transformation in the tumor and TME, we performed additional studies to analyze the impact of the combinatorial treatment further. Transcriptomic analyses showed a tumor cell enrichment in the expression of genes that are downregulated in glioma stem cells and upregulated in oligodendrocyte differentiation[42,43] (Figure 6A). Regarding TME reshaping, TCR and IFNγ pathways, and cytokine and inflammatory response are significantly augmented in the combination (Figure 6B). Interestingly, additional analyses showed an augmented infiltration in all the subtypes of dendritic cells in Delta-24-RGD/ONC201 cotreatment (Figure 6C–D). Further analyses of the phenotype of the relevant immune populations were performed. Conventional $CD4^+$ T cells of mice treated with the combination showed higher expression of CD69, PD-1, and Ki67, indicating a more activated and proliferative profile compared with the single treatments (Figure 6E). Interestingly, the percentage of this population that express the zinc-finger protein Helios, which have been previously associated with differentiation of this population to type 2 T helper,[44] was also bigger in mice treated with the combination (Figure 6E). Analysis of Treg cells did not show differences in the studied phenotype markers (Supplementary Figure S12B). Regarding $CD8^+$ T cells, significant activation was found through an increase in the $CD69^+$ population in mice that received the combination. Of note, more than 90% of $CD8^+$T cells in the tumors of all the groups expressed Ki67, indicating a proliferating state, except for the ONC201 group (Figure 6F). Interestingly, phenotypic characterization of the myeloid compartment showed no differences between conditions (Supplementary Figure S12C–E).

We also wanted to check the state of the tumor microenvironment at delayed time points from ONC201 administration. Interestingly, a significant augmented immune recruitment in the Delta-24-RGD groups was observed, but ONC201 addition did not lead to significant changes (Supplementary Figure S13). These results suggest that the clearance of ONC201 several days after administration could play a role in tumor microenvironment remodeling.

In summary, these findings underscore the fact that the therapeutic benefit of the combination treatment is, at least partially, due to a substantial immune response against tumors.

Discussion

Unfortunately, as of today, pHGGs and DMGs persist as incurable diseases despite improvements in therapeutic regimens, and outcomes remain almost inalterable without clinical benefits,[46] which highlights the urgent need to uncover efficacious treatments. The imipridone ONC201

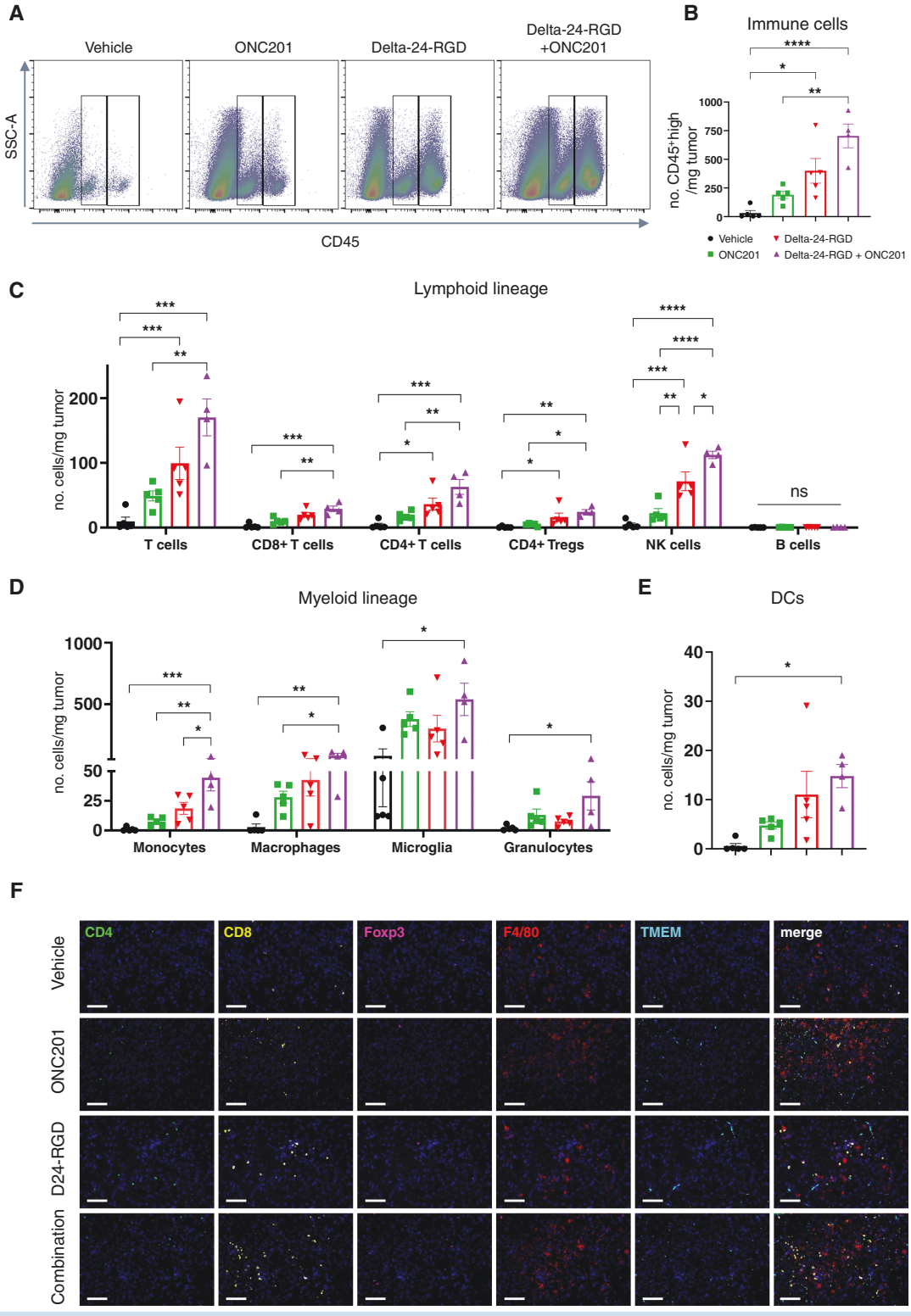

Figure 5. (A) Dot plot examples of CD45⁺middle (ie, microglia, left box) and CD45⁺high (remaining immune cells, right box) stained cells 7 days after each treatment in XFM-bearing mice, analyzed by flow cytometry. (B) Quantification of CD45⁺high stained cells 7 days after each treatment in XFM-bearing mice. (C) Quantification of lymphoid lineage (B cells, total T cells, NK cells, CD4⁺ T cells, CD8⁺ T cells, and CD4⁺ Treg cells). (D) Quantification of myeloid lineage (monocytes, macrophages, microglia, and granulocytes). (E) Quantification of dendritic cells. For B–E, data are shown as the mean ± SEM and expressed as the number of cells/mg tumor. At least 4 animals were included per group. One-way ANOVA was performed for statistical analysis. *$P < .05$, **$P < .01$, ***$P < .001$, ****$P < .0001$, ns, not significant. (F) Representative micrographs of multiplexed immunofluorescence in XFM-bearing mice tumors 7 days after each treatment immunofluorescence analysis to detect the following cell markers: CD4, CD8, Foxp3, F4/80 and TMEM119. The nuclei were counterstained with DAPI. Scale bars: 100 µm.

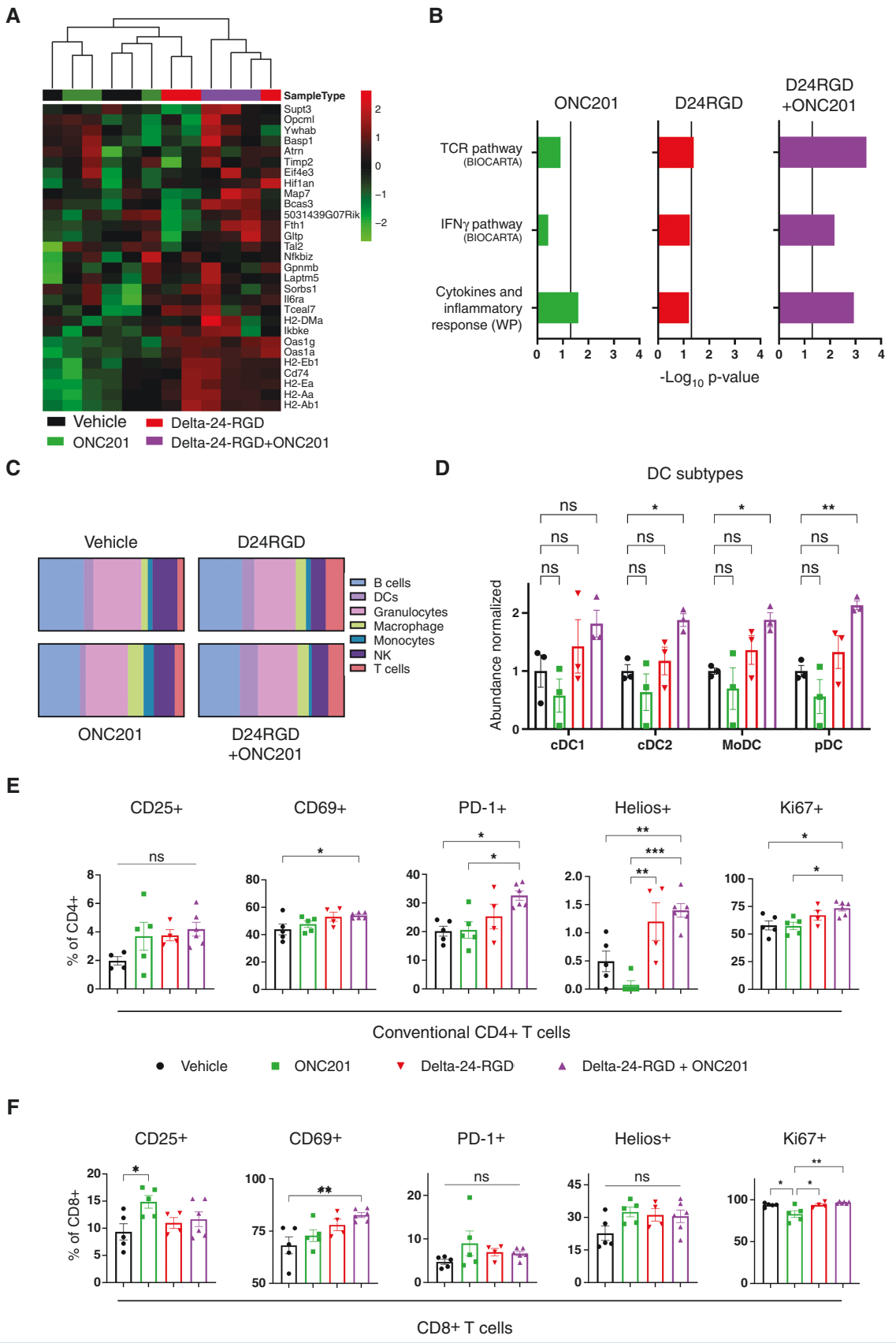

Figure 6. (A) Heatmap and hierarchical clustering represent the differential expression in genes that are downregulated in glioma stem cells and upregulated in oligodendrocyte differentiation.[42,43] Transcriptomic data were obtained from XFM-bearing mice tumors after 7 days of each

treatment. Three mice were included per group. (B) GSEA of transcriptomic signatures in treated XFM-bearing mice tumors compared with vehicle-bearing mice. Vertical line indicates statistical significance ($-Log_{10}$ 0.05). (C) Relative abundances (in percentages) of the different immune populations were determined by analysis of RNAseq data through the online tool ImmuCellAI-mouse.[45] (D) Normalized abundance of type-1 and 2 conventional DCs (cDC1/2), monocyte-derived DCs (moDC), and plasmacytoid DCs (pDC). E and F. Percentage of positive populations of the indicated markers in conventional $CD4^+$ T cells (E) and $CD8^+$ cells (F). Immune cells were analyzed 7 days after each treatment in XFM-bearing mice and measured by flow cytometry. For D, E, and F, data are shown as the mean ± SEM, and at least 3 animals were included per group. One-way ANOVA was performed for statistical analysis. $^*P < .05$, $^{**}P < .01$, $^{***}P < .001$, ns, not significant.

and the oncolytic adenovirus Delta-24-RGD are two promising drugs in the field that have already been tested in pediatric clinical trials. ONC201 has shown a degree of efficacy in DMG pediatric patients,[27] and a phase III study (NCT05580562) is now active and recruiting. Regarding Delta-24-RGD, our group previously showed the safety and antitumor effects in preclinical[16,17] and clinical studies[13] in these tumor types. Despite the encouraging results of these two agents, neither of them led to total tumor eradication. Thus, the idea of combining these two promising therapies for potential translation in the clinic is certainly appealing. Indeed, ONC201 has been combined with other strategies to enhance its efficacy, such as radiation,[47] anti-angiogenic agents,[48] or other small molecules.[49–51] Strikingly in the DMG field, ONC201 in combination with paxalisib, a PI3K/Akt inhibitor, showed promising results in preclinical and clinical applications.[37]

Another fact that supports the application of the Delta-24-RGD/ONC201 combination is the low rate of adverse events resulting from these agents. Both drugs showed a safe, nontoxic clinical profile.[13,31,32,52,53] Intratumoral administration of Delta-24-RGD (DNX-2401) led to grades 1–2 events, with sporadic grade 3 events.[13] Similarly, ONC201 is well tolerated by patients, and no adverse events ≥2 were found in diverse clinical trials.[31,32,52,53]

In this work, we showed the feasibility and superior therapeutic efficacy of the Delta-24-RGD/ONC201 combination in pHGGs and DMGs. Although it is unclear whether a higher efficacy correlates with the H3 mutational status due to the limited number of cell lines evaluated in this work, this combination has the potential to reach a wider range of patients. This is very interesting because in the last phase III ONC201 clinical trial, DIPG tumors, located in the pons, were excluded, and these patients could benefit from combination treatment. Furthermore, this new regime could be applied to those patients at recurrence for whom RT is not an option. One issue regarding the Delta-24-RGD/ONC201 combination was the ability of ONC201 to suppress cellular metabolism and disrupt mitochondrial activity,[24–30] which in turn could affect virus viability and thus antitumor effects. Our data ruled out the negative impact of ONC201 on viral replication and highlighted the ability of the combination to induce DNA damage to drive the improved antiglioma effect. This ultimately led to an increase in cell death, likely enabling antigen presentation to improve the antitumor immune response.

Interestingly, both Delta-24-RGD and ONC201 trigger an antitumoral immune response.[13,16,20,30,32] ONC201 increased the infiltration and activation of NK cells in a preclinical colon model.[30] Moreover, in an adult patient cohort with advanced solid tumors, including prostate, colon, endometrial cancer, and glioblastoma, treatment with ONC201 was associated with the infiltration and activation of NK cells, as well as induction of immune cytokines and effectors.[32] However, ONC201's effect on the immune response in pediatric brain tumors is still unknown, although several groups are currently working on evaluating this aspect. We previously showed that Delta-24-RGD primarily triggers $CD4^+$ and $CD8^+$ T-cell infiltration[13,16,20] among other immune populations. Here, we show that the combination of ONC201 and Delta-24-RGD seemed to increase the abundance of both lymphoid and myeloid populations in tumors. Importantly, Delta-24-RGD/ONC201 produces a higher activation and proliferation in $CD4^+$ T cells and a higher activation in $CD8^+$ T cells. However, immunocompetent models treated with the combination showed a subtle improvement in survival advantage, although not as much of an improvement as their immunosuppressed counterparts using a human-derived xenograft. This could be because the replication of serotype 5 adenoviruses is hindered in murine cells,[41] and the adenovirus effect is restricted to only infection and protein production without effective replication. Thus, the observed effect could be somehow attenuated. This limitation should be resolved in a patient setting, in which not only would the adenovirus be able to replicate and exert its oncolytic capacity, but it would also trigger immune activation against the tumor. Additionally, the effects of ONC201 on immune cells that are still present in the nude and NSG BALB/c immunosuppressed models used in the work, such as the aforementioned NK cells, neutrophils, monocytes, and macrophages, could play a role. Indeed, macrophages have been suggested to be reprogrammed by ONC201 toward a proinflammatory status.[54] Although we did not find any differences in the phenotype in the myeloid compartment, we cannot rule out the possibility that the schedule or timing of the experiment could yield different results. Thus, further research is needed to completely elucidate the impact of ONC201 on immune populations that have been recruited by the oncolytic virus in a human context. In summary, we showed that the Delta-24-RGD/ONC201 combination had superior efficacy compared to either agent alone, and this difference can be explained, at least partially, by the increase in DNA damage and the antitumor immune response. Therefore, the results of this study support the evaluation of Delta-24-RGD/ONC201 in future clinical trials for pHGGs, including DMGs, regardless of tumor location or mutation status.

Supplementary material

Supplementary material is available online at *Neuro-Oncology* (https://academic.oup.com/neuro-oncology).

Keywords

DMGs | Delta-24-RGD | immunovirotherapy | ONC201 | pHGGs

Funding

The performed work was supported through a Predoctoral Fellowship from Instituto de Salud Carlos III (FI20/00020; DdlN), a Predoctoral Fellowship from Gobierno de Navarra (VL), by an FPU (FPU21/00603) grant from Ministerio de Universidades, Gobierno de España (RHO), and a Postdoctoral Fellowship ChadTough-Defeat DIPG (MGM). Plan de colaboración Internacional (PCI2021-122084-2B) Spanish Ministry of Science and Innovation (SL). GRANATE project funded by the Government of Navarre in the frame of "Proyectos Estratégicos de I+D 2022-2025, Reto GEMA (001-1411-2022-000066)" (MMA, APG, SL). ChadTough-Defeat DIPG (MMA), AECC General Projects (PRYGN21937; MMA), Instituto de Salud Carlos III y Fondos Feder (PI19/01896 MMA, PI18/00164 APG "A way to make Europe"); Fundación La Caixa/Caja Navarra (APG and MMA); Fundación El sueño de Vicky; Asociación Pablo Ugarte-Fuerza Julen; Fundación ADEY; Fundación ACS; Fundación Hay que tomarse la vida con tumor (JGP-L, APG and MMA); Fundación Blanca Morell (SL; JGP-L); Fundación + Investigación + Vida (La Guareña); Red Española de Terapias Avanzadas TERAV ISCIII (RD21/0001/0022; funded by Unión Europea-Next Generation EU. Plan de Recuperación Transformación y Resiliencia). This project also received funding from the European Research Council under the European Union´s Horizon 2020 Research and Innovation Programme (817884 ViroPedTher to MMA).

Conflict of interest statement

JEA is an employee and shareholder of Chimerix and has ownership (including patents) regarding ONC201. The rest of the authors do not have potential conflicts of interest to disclose.

Authorship statement

Conception and design of the study: DdlN, MMA. Acquisition, analysis, and/or interpretation of data: All authors. Writing-original draft preparation: DdlN, MMA. Writing-review and editing: All authors. Study supervision: MMA. All authors discussed and reviewed the manuscript and approved the manuscript for publication.

Data availability

RNAseq data have been deposited in GEO and are available as of the date of publication. The data that support the findings of this study are available within the paper or Supplementary Information. Source data files are available from the corresponding author upon request.

Affiliations

Health Research Institute of Navarra (IdiSNA), Pamplona, Spain (D.N., I.A.-M., V.L., M.G.-H., A.L., N.C., M.Z., L.M., M.G.-M., M.C.O., A.C.T.-C., R.H.-O., J.M.-S., L.D., I.H.-C., M.H., E.G., J.G.P.-L., A.P.-G., S.L., M.M.A.); Solid Tumor Program, Center for the Applied Medical Research, Pamplona, Spain (D.N., I.A.-M., V.L., M.G.-H., A.L., N.C., M.Z., L.M., M.G.-M., M.C.O., A.C.T.-C., R.H.-O., J.M.-S., L.D., I.H.-C., J.G.P.-L., A.P.-G., S.L., M.M.A.); Department of Pediatrics, Clínica Universidad de Navarra, Pamplona, Spain (D.N., I.A.-M., V.L., M.G.-H., A.L., N.C., M.Z., L.M., M.G.-M., M.C.O., R.H.-O., J.M.-S., L.D., I.H.-C., A.P.-G., S.L., M.M.A.); Department of Neuro-Oncology, The University of Texas MD Anderson Cancer Center, Houston, Texas, USA (M.G.-M., J.F., C.G.-M.); Jack Martin Fund Division of Pediatric Hematology-oncology, Mount Sinai, New York, USA (O.J.B., J.L.); Children's National Health System, Center for Genetic Medicine Research, Washington, District of Columbia, USA (J.N.); Virginia Tech University, Washington, District of Columbia, USA (J.N.); Division of Oncology and Children's Research Center, DIPG/DMG Research Center Zurich, University Children's Hospital Zurich, Zurich, Switzerland (J.N., S.M.); University of California, San Francisco; San Francisco, California, USA (S.M.); Division of Pharmaceutical Sciences, James L. Winkle College of Pharmacy, University of Cincinnati, Cincinnati, Ohio, USA (T.N.P.); Princess Máxima Center for Pediatric Oncology, Utrecht, The Netherlands (J.v.d.L.); Bioinformatics Platform, Center for Applied Medical Research, University of Navarra (CIMA), Pamplona, Spain (M.H., E.G.); Department of Pediatrics, University of Michigan, Ann Arbor, Michigan, USA (C.K., S.V.); Chimerix, Inc. Durham, North Carolina, USA (J.E.A.); Cancer Signalling Research Group, School of Biomedical Sciences and Pharmacy, College of Health, Medicine and Wellbeing, University of Newcastle, Callaghan, New South Wales, Australia (M.D.D.); Precision Medicine Research Program, Hunter Medical Research Institute, New Lambton Heights, New South Wales, Australia (M.D.D.); Paediatric Stream, Mark Hughes Foundation Centre for Brain Cancer Research, College of Health, Medicine, and Wellbeing, Callaghan, New South Wales, Australia (M.D.D.); Department of Neurology, Clínica Universidad de Navarra, Pamplona, Spain (J.G.P.-L.)

References

1. Ostrom QT, Price M, Neff C, et al. CBTRUS statistical report: Primary brain and other central nervous system tumors diagnosed in the United States in 2015-2019. *Neuro Oncol*. 2022;24(5):v1–v95.
2. Cooney T, Lane A, Bartels U, et al. Contemporary survival endpoints: An international diffuse intrinsic pontine glioma registry study. *Neuro Oncol*. 2017;19(9):1279–1280.
3. Kline C, Felton E, Allen IE, Tahir P, Mueller S. Survival outcomes in pediatric recurrent high-grade glioma: Results of a 20-year systematic review and meta-analysis. *J Neurooncol*. 2018;137(1):103–110.

4. Pfister SM, Reyes-Múgica M, Chan JKC, et al. A summary of the inaugural WHO classification of pediatric tumors: Transitioning from the optical into the molecular era. *Cancer Discov.* 2022;12(2):331–355.
5. Mackay A, Burford A, Carvalho D, et al. Integrated molecular meta-analysis of 1,000 pediatric high-grade and diffuse intrinsic pontine glioma. *Cancer Cell.* 2017;32(4):520–537.e5.
6. Jones C, Karajannis MA, Jones DTW, et al. Pediatric high-grade glioma: Biologically and clinically in need of new thinking. *Neuro Oncol.* 2017;19(2):153–161.
7. Pui CH, Gajjar AJ, Kane JR, Qaddoumi IA, Pappo AS. Challenging issues in pediatric oncology. *Nat Rev Clin Oncol.* 2011;8(9):540–549.
8. Horbinski C, Berger T, Packer RJ, Wen PY. Clinical implications of the 2021 edition of the WHO classification of central nervous system tumours. *Nat Rev Neurol.* 2022;18(9):515–529.
9. Hoffman LM, Van Zanten SEMV, Colditz N, et al. Clinical, radiologic, pathologic, and molecular characteristics of long-term survivors of Diffuse Intrinsic Pontine Glioma (DIPG): A collaborative report from the International and European Society for Pediatric Oncology DIPG registries. *J Clin Oncol.* 2018;36(19):1963–1972.
10. Dunkel IJ, Doz F, Foreman NK, et al. Nivolumab with or without ipilimumab in pediatric patients with high-grade CNS malignancies: Safety, efficacy, biomarker, and pharmacokinetics—CheckMate 908. *Neuro Oncol.* 2023;25(8):1530–1545.
11. Vitanza NA, Wilson AL, Huang W, et al. Intraventricular B7-H3 CAR T cells for diffuse intrinsic pontine glioma: Preliminary first-in-human bioactivity and safety. *Cancer Discov.* 2023;13(1):114–131.
12. Majzner RG, Ramakrishna S, Yeom KW, et al. GD2-CAR T cell therapy for H3K27M-mutated diffuse midline gliomas. *Nature.* 2022;603(7903):934–941.
13. Gállego Pérez-Larraya J, Garcia-Moure M, Labiano S, et al. Oncolytic DNX-2401 virus for pediatric diffuse intrinsic pontine glioma. *N Engl J Med.* 2022;386(26):2471–2481.
14. Friedman GK, Johnston JM, Bag AK, et al. Oncolytic HSV-1 G207 immunovirotherapy for pediatric high-grade gliomas. *N Engl J Med.* 2021;384(17):1613–1622.
15. Kaufman HL, Kohlhapp FJ, Zloza A. Oncolytic viruses: A new class of immunotherapy drugs. *Nat Rev Drug Discov.* 2015;14(9):642–662.
16. Martínez-Vélez N, Garcia-Moure M, Marigil M, et al. The oncolytic virus Delta-24-RGD elicits an antitumor effect in pediatric glioma and DIPG mouse models. *Nat Commun.* 2019;10(1):2235.
17. Martinez-Velez N, Marigil M, García-Moure M, et al. Delta-24-RGD combined with radiotherapy exerts a potent antitumor effect in diffuse intrinsic pontine glioma and pediatric high grade glioma models. *Acta Neuropathol Commun.* 2019;7(1):1–12.
18. Lang FF, Conrad C, Gomez-Manzano C, et al. Phase I study of DNX-2401 (delta-24-RGD) oncolytic adenovirus: Replication and immunotherapeutic effects in recurrent malignant glioma. *J Clin Oncol.* 2018;36(14):1419–1427.
19. Nassiri F, Patil V, Yefet LS, et al. Oncolytic DNX-2401 virotherapy plus pembrolizumab in recurrent glioblastoma: a phase 1/2 trial. *Nat Med.* 2023;29(6):1370–1378.
20. Garcia-Moure M, Gonzalez-Huarriz M, Labiano S, et al. Delta-24-RGD, an oncolytic adenovirus, increases survival and promotes proinflammatory immune landscape remodeling in models of AT/RT and CNS-PNET. *Clin Cancer Res.* 2021;27(6):1807–1820.
21. Fueyo J, Alemany R, Gomez-Manzano C, et al. Preclinical characterization of the antiglioma activity of a tropism-enhanced adenovirus targeted to the retinoblastoma pathway. *J Natl Cancer Inst.* 2003;95(9):652–660.
22. Jackson ER, Persson ML, Fish CJ, et al. A review of the anti-tumor potential of current therapeutics targeting the mitochondrial protease ClpP in H3K27-altered, diffuse midline glioma. *Neuro Oncol.* 2023:noad144; Online ahead of print. doi:10.1093/neuonc/noad144.
23. Madhukar NS, Khade PK, Huang L, et al. A Bayesian machine learning approach for drug target identification using diverse data types. *Nat Commun.* 2019;10(1):1–14.
24. Przystal JM, Cianciolo Cosentino C, Yadavilli S, et al. Imipridones affect tumor bioenergetics and promote cell lineage differentiation in diffuse midline gliomas. *Neuro Oncol.* 2022;24(9):1438–1451.
25. Ishizawa J, Zarabi SF, Davis RE, et al. Mitochondrial ClpP-mediated proteolysis induces selective cancer cell lethality. *Cancer Cell.* 2019;35(5):721–737.e9.
26. Duchatel RJ, Mannan A, Woldu AS, et al. Preclinical and clinical evaluation of German-sourced ONC201 for the treatment of H3K27M-mutant diffuse intrinsic pontine glioma. *Neuro Oncol Adv.* 2021;3(1):1–12.
27. Venneti S, Kawakibi AR, Ji S, et al. Clinical efficacy of ONC201 in H3K27M- mutant diffuse midline gliomas is driven by disruption of integrated metabolic and epigenetic pathways. *Cancer Discov.* 2023;13(11):2370–2393.
28. Kline CLB, Van Den Heuvel APJ, Allen JE, et al. ONC201 kills solid tumor cells by triggering an integrated stress response dependent on ATF4 activation by specific eIF2a kinases. *Sci Signal.* 2016;9(415):1–11.
29. Ishizawa J, Kojima K, Chachad D, et al. ATF4 induction through an atypical integrated stress response to ONC201 triggers p53-independent apoptosis in hematological malignancies. *Sci Signal.* 2016;9(415):1–15.
30. Wagner J, Leah Kline C, Zhou L, et al. Dose intensification of TRAIL-inducing ONC201 inhibits metastasis and promotes intratumoral NK cell recruitment. *J Clin Invest.* 2018;128(6):2325–2338.
31. Arrillaga-Romany I, Odia Y, Prabhu VV, et al. Biological activity of weekly ONC201 in adult recurrent glioblastoma patients. *Neuro Oncol.* 2020;22(1):94–102.
32. Stein MN, Malhotra J, Tarapore RS, et al. Safety and enhanced immunostimulatory activity of the DRD2 antagonist ONC201 in advanced solid tumor patients with weekly oral administration. *J ImmunoTher Cancer.* 2019;7(1):1–9.
33. Halvorson KG, Barton KL, Schroeder K, et al. A high-throughput in Vitro drug screen in a genetically engineered mouse model of diffuse intrinsic pontine glioma identifies BMS-754807 as a promising therapeutic agent. *PLoS One.* 2015;10(3):e0118926–e0118916.
34. Barton KL, Misuraca K, Cordero F, et al. PD-0332991, a CDK4/6 inhibitor, significantly prolongs survival in a genetically engineered mouse model of brainstem glioma. *PLoS One.* 2013;8(10):e77639–e77637.
35. Du Chatinier A, Meel MH, Das AI, et al. Generation of immunocompetent syngeneic allograft mouse models for pediatric diffuse midline glioma. *Neuro Oncol Adv.* 2022;4(1):1–12.
36. Ianevski A, Giri AK, Aittokallio T. SynergyFinder 3.0: An interactive analysis and consensus interpretation of multi-drug synergies across multiple samples. *Nucleic Acids Res.* 2022;50(W1):W739–W743.
37. Jackson ER, Duchatel RJ, Staudt DE, et al. ONC201 in combination with paxalisib for the treatment of H3K27-altered diffuse midline glioma. *Cancer Res.* 2023:OF1–OF17. Online ahead of print.
38. De Billy E, Pellegrino M, Orlando D, et al. Dual IGF1R/IR inhibitors in combination with GD2-CAR T-cells display a potent anti-tumor activity in diffuse midline glioma H3K27M-mutant. *Neuro Oncol.* 2022;24(7):1150–1163.
39. Arunachalam S, Szlachta K, Brady SW, et al. Convergent evolution and multi-wave clonal invasion in H3 K27-altered diffuse midline gliomas treated with a PDGFR inhibitor. *Acta Neuropathol Commun.* 2022;10(1):1–14.
40. Karen KA, Hearing P. Adenovirus core protein VII protects the viral genome from a DNA damage response at early times after infection. *J Virol.* 2011;85(9):4135–4142.
41. Blair GE, Dixon SC, Griffiths SA, Blair Zajdel ME. Restricted replication of human adenovirus type 5 in mouse cell lines. *Virus Res.* 1989;14(4):339–346.

42. Beier D, Hau P, Proescholdt M, et al. CD133+ and CD133- glioblastoma-derived cancer stem cells show differential growth characteristics and molecular profiles. *Cancer Res*. 2007;67(9):4010–4015.
43. Pescini Gobert R, Joubert L, Curchod M-L, et al. Convergent functional genomics of oligodendrocyte differentiation identifies multiple autoinhibitory signaling circuits. *Mol Cell Biol*. 2009;29(6):1538–1553.
44. Serre K, Bénézech C, Desanti G, et al. Helios is associated with CD4 T cells differentiating to T helper 2 and follicular helper T cells in vivo independently of Foxp3 expression. *PLoS One*. 2011;6(6):e20731.
45. Miao YR, Xia M, Luo M, et al. ImmuCellAI-mouse: A tool for comprehensive prediction of mouse immune cell abundance and immune microenvironment depiction. *Bioinformatics*. 2022;38(3):785–791.
46. MacDonald TJ, Aguilera D, Kramm CM. Treatment of high-grade glioma in children and adolescents. *Neuro Oncol*. 2011;13(10):1049–1058.
47. He L, Bhat K, Ioannidis A, et al. Effects of the DRD2/3 antagonist ONC201 and radiation in glioblastoma. *Radiother Oncol*. 2021;161:140–147.
48. Wagner J, Kline CL, Zhou L, Khazak V, El-Deiry WS. Anti-tumor effects of ONC201 in combination with VEGF-inhibitors significantly impacts colorectal cancer growth and survival in vivo through complementary non-overlapping mechanisms. *J Exp Clin Cancer Res*. 2018;37(1):1–12.
49. Liguori NR, Sanchez Sevilla Uruchurtu A, Zhang L, et al. Preclinical studies with ONC201/TIC10 and lurbinectedin as a novel combination therapy in small cell lung cancer (SCLC). *Am J Cancer Res*. 2022;12(2):729–743.
50. Prabhu VV, Talekar MK, Lulla AR, et al. Single agent and synergistic combinatorial efficacy of first-in-class small molecule imipridone ONC201 in hematological malignancies. *Cell Cycle*. 2018;17(4):468–478.
51. Di Cristofano FR, Fong MW, Huntington KE, et al. Synergistic activity of ABT-263 and ONC201/TIC10 against solid tumor cell lines is associated with suppression of anti-apoptotic Mcl-1, BAG3, pAkt, and upregulation of pro-apoptotic Noxa and Bax cleavage during apoptosis. *Am J Cancer Res*. 2023;13(1):307–325. www.ajcr.us/
52. Anderson PM, Trucco MM, Tarapore RS, et al. Phase II Study of ONC201 in neuroendocrine tumors including pheochromocytoma-paraganglioma and desmoplastic small round cell tumor. *Clin Cancer Res*. 2022;28(9):1773–1782.
53. Stein MN, Bertino JR, Kaufman HL, et al. First-in-human clinical trial of oral ONC201 in patients with refractory solid tumors. *Clin Cancer Res*. 2017;23(15):4163–4169.
54. Geiß C, Witzler C, Poschet G, Ruf W, Régnier-Vigouroux A. Metabolic and inflammatory reprogramming of macrophages by ONC201 translates in a pro-inflammatory environment even in presence of glioblastoma cells. *Eur J Immunol*. 2021;51(5):1246–1261.